Binding of NH_3 to graphite and to a (9,0) carbon nanotube

Charles W. Bauschlicher, Jr. and Alessandra Ricca
Mail Stop 230-3, NASA Ames Center for Nanotechnology,
NASA Ames Research Center, Moffett Field, California 94035, USA
(Received 12 February 2004; published 14 September 2004)

The interaction of NH_3 with graphite and a (9,0) carbon nanotube is studied using the second-order Møller-Plesset and density functional theory approaches. For both graphite and the nanotube, our best estimate of the NH_3 binding energy is 2 ± 2 kcal/mol. NH_3 physisorbs on the carbon surface and the hydrogen end points toward the carbon surface. The binding is mostly electrostatic in nature and there is very little charge transfer occurring. Band-structure calculations on a (10,0) semiconducting nanotube show essentially no change in the nanotube band gap when NH_3 is added. The implications of these calculations on the experimental results are discussed.

DOI: 10.1103/PhysRevB.70.115409 PACS number(s): 61.46.+w, 68.43.Bc, 68.43.Fg

I. INTRODUCTION

Chemical sensors based on single-walled carbon nanotubes (SWCNTs) are gaining considerable interest due to their very high sensitivity towards gaseous molecules, such as O_2, NH_3, NO_2, SO_2, etc. A concerted effort between experiment and theory is beginning to unravel the mechanism by which SWCNT-based chemical sensors operate.

In the case of O_2, experiments[1,2] in conjunction with theoretical studies[3–6] support the conclusion that O_2 does not dope SWCNTs and does not affect the electronic spectra of SWCNTs. For nanotube field-effect transistors (NT-FETs) formed by a single tube, Avouris and co-workers[7–9] have conclusively demonstrated that the adsorption of O_2 at the nanotube/metal junction is responsible for the change in transport properties, and a detailed theoretical phenomenological model of the modulation of the Schottky barrier by O_2 at the SWCNT/metal interface has been obtained recently by Yamada.[10] For nanotube bundles and thin films, Goldoni *et al.*[2] have shown that residual contaminants, such as Na and catalyst particles, remain even after annealing cycles in ultrahigh vacuum and these contaminants may be responsible for the reported sensitivity to O_2, as reported by Collins *et al.*[11] The removal of these contaminants makes the electronic spectra insensitive to O_2.[2]

In the case of NH_3 the experiment reported by Kong *et al.*[12] on an individual semiconducting SWCNT showed that the conductance of the SWCNT sample decreases by approximately 100-fold after exposure to a flow of Ar or air containing 1% NH_3. The authors suggested that a charge transfer from NH_3 to SWCNTs is responsible for the change in properties of the SWCNTs. Recently, however, Bradley *et al.*[13] have shown that NT-FETs that have been heated in vacuum are not sensitive to ammonia, but NT-FETs respond to ammonia gas only when they are in ambient (humid conditions). The authors conclude that ammonia does not dope nanotubes directly, but dissolves in water instead, and the ammonia-water solution charges the NT-FETs. Bradley *et al.*[14] have also shown experimentally that protecting the metal-nanotube contacts from NH_3 exposure by a passivation layer changes the sensitivity by only a few percent, which implies that the sensing is not dominated by the contact region, as is the case for O_2, but by the carbon nanotube region. On the other hand, Goldoni *et al.*[2] report that exposure of a clean SWCNT bundle after annealing up to 1800 K to NH_3 changes the C 1s peak in carbon photoemission and they explain this feature by saying that NH_3 molecules act as charge donors. The experiments of Bradley *et al.* and those of Goldoni *et al.* are only consistent if there is water vapor present in the experiments of Goldoni *et al.*

The few theoretical studies published in the literature[15,16] support a charge transfer of 0.03–0.04 electrons with NH_3 donating to the SWCNT. Both theoretical works are based on the local density approximation (LDA) approach, which is known to overestimate the binding energy, and therefore, the charge transfer. Moreover, the use of plane-wave basis sets is prone to basis set superposition errors (BSSE) that can lead to serious problems for the description of a weakly bound system.

In the present work we want to reevaluate the binding of NH_3 to SWCNTs and assess if NH_3 dopes the SWCNTs. The results of our work could help resolve the controversies regarding the sensing of NH_3 by carbon nanotubes.

II. MODELS AND METHODS

Most of the calculations are performed using the second-order Møller-Plesset (MP2) perturbation theory. Since the binding is found to be weak, we correct the bond energies for BSSE using the counterpoise approach. To calibrate the MP2 level, one calculation is performed using the coupled cluster singles and doubles approach,[17] including the effect of connected triples determined using perturbation theory,[18] CCSD(T). Density functional theory (DFT) (using the B3LYP[19] hybrid[20] functional) is used to compare the effect of the model size on the binding energies. The basis sets that are used are those developed by Pople and co-workers,[21] or those developed by Dunning and co-workers.[22,23] The MP2 and B3LYP calculations are performed using GAUSSIAN98,[24] while the CCSSD(T) calculations were performed using

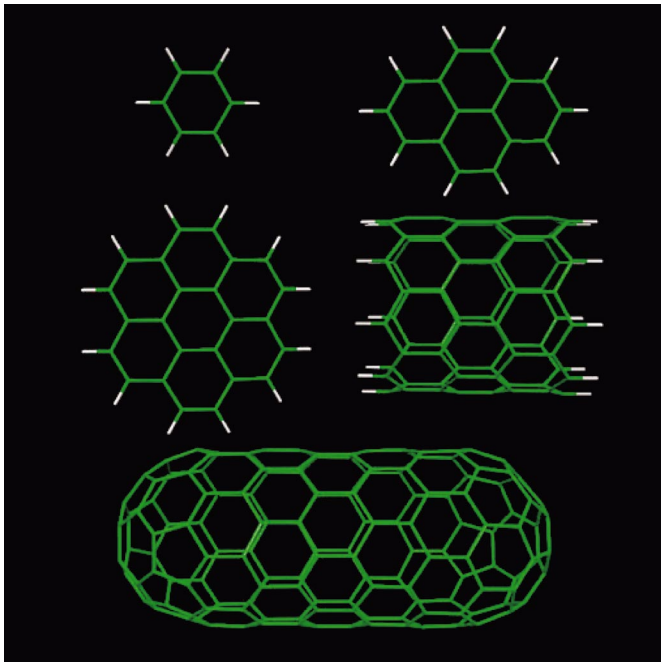

FIG. 1. (Color) The models used in this work.

MOLPRO.[25]

We use several models for the carbon nanotube and graphite, which are shown in Fig. 1. The models for graphite are benzene (C_6H_6), pyrene ($C_{16}H_{10}$), and coronene ($C_{24}H_{12}$). These species are fully optimized with and without NH_3; the free systems are planar and when NH_3 is added, the benzene, pyrene, and coronene components are very close to planar. A curved coronene is used to model a (9,0) nanotube. In the geometry optimization, the positions of the carbon atoms of the curved coronene are fixed at those derived from a free (9,0) tube, and only the NH_3 geometry and its position above the tube are optimized. In addition to not optimizing the position of the carbons, the C-H bonds are colinear with the original C-C bonds, and the C-H bond lengths are fixed at 1.084 Å.

The two largest models of the (9,0) tube are the $C_{78}H_{18}$ ring with C-H bonds to terminate the dangling bonds, and a C_{150} tube with two caps. In these two models, the species with and without NH_3 are fully optimized, since the models naturally retain their curvature.

We also perform DFT periodic-boundary-condition calculations with a plane-wave basis on a (10,0) tube interacting with NH_3 using the CASTEP program.[26,27] We use the generalized gradient approximation in conjunction with the functional developed by Perdew, Burke, and Ernzerhof.[28] The kinetic energy cutoff is taken as 310.0 eV (Fourier transform grid $72\times72\times45$). The Brillouin zone is sampled using a $2\times2\times2$ Monkhorst-Pack mesh (four k points). All the atoms are treated using the default ultrasoft pseudopotentials provided by the CASTEP program. We use the supercell shown in Fig. 2, which is periodic along the z axis with cell parameters $a=14.0$ Å, $b=14.0$ Å, $c=8.452$ Å, $\alpha=90°$, $\beta=90°$, and $\gamma=120°$. The optimal NH_3 position above the tube is taken from our MP2 calculations.

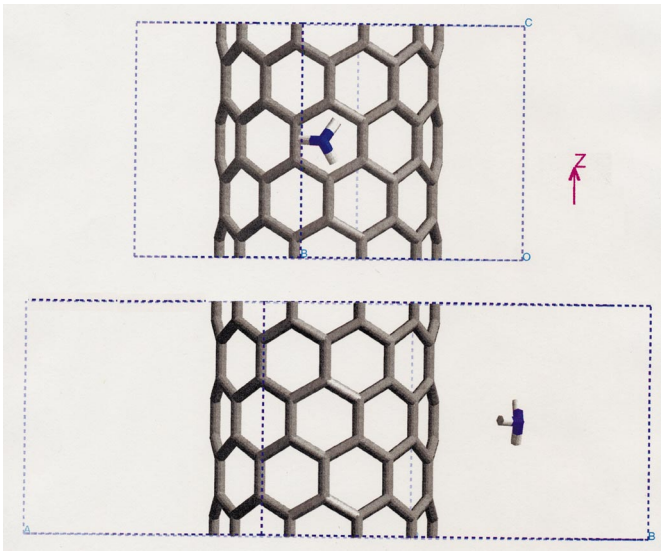

FIG. 2. (Color) Periodic cell containing a (10,0) tube and a physisorbed NH_3 molecule. The periodicity is along the axis of the tube (z axis).

III. RESULTS AND DISCUSSION

We first consider the C_6H_6 model for graphite. The free C_6H_6 is planar and its geometry is hardly affected by the

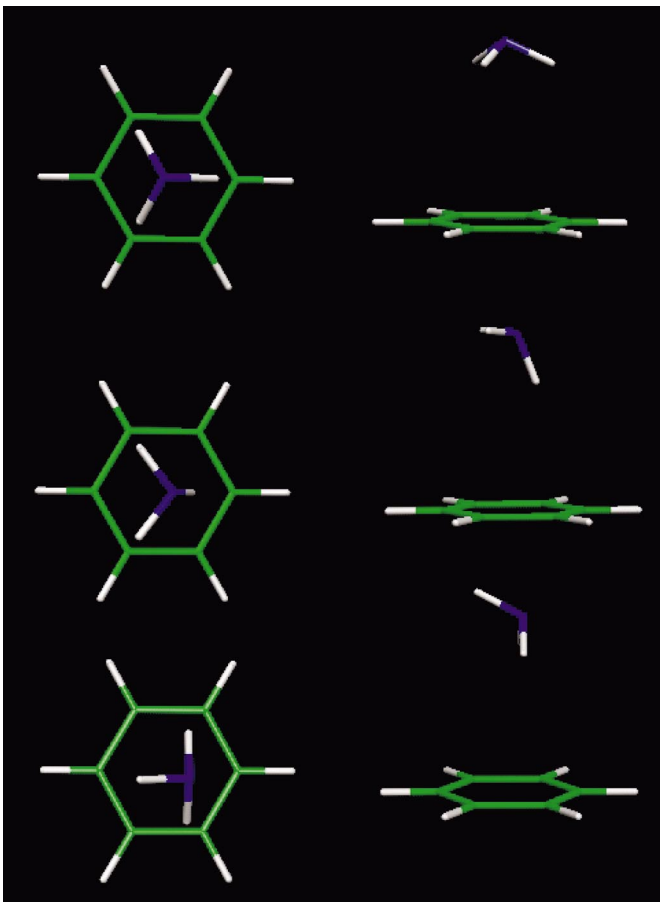

FIG. 3. (Color) The MP2/6-31G* optimized geometry for C_6H_6-NH_3.

TABLE I. NH_3 binding energy, in kcal/mol, computed using the MP2 level of theory.

Model	D_e	D_e-BSSE	Scaled[a]
Planar C_6H_6 model, perpendicular C_{3v} symmetry			
6-31G*	2.53	0.50	0.41
6-31+G*	2.48	0.76	0.63
6-311G(2*df*,2*p*)	3.34	1.35	1.13
aug-cc-pVTZ	2.50	1.93	1.61
Planar C_6H_6 model, tilted two H atoms down			
6-31G*	2.68	1.04	0.86
6-311G(2*df*,2*p*)	3.39	1.91	1.59
aug-cc-pVTZ	3.04	2.41	2.01
Planar C_6H_6 model, tilted one H atom down			
6-31G*	2.74	0.91	0.76
6-31+G*	3.02	1.08	0.90
6-31G(2*d*,*p*)	3.01	1.35	1.13
6-311G(2*df*,2*p*)	3.66	1.91	1.59
6-311+G(2*df*,2*p*)	2.89	2.11	1.76
aug-cc-pVTZ	3.17	2.42	2.02
Planar $C_{24}H_{12}$ model, perpendicular			
6-31G*	3.72	1.26	1.05
6-31G(2*d*,*p*)	4.57	1.98	1.65
Planar $C_{24}H_{12}$ model, tilted[b]			
6-31G*	3.26	1.51	1.26
6-31G(2*d*,*p*)	4.08	2.25	1.88
Curved $C_{24}H_{12}$ model, perpendicular			
6-31G*	3.60	0.79	0.66
6-31G(2*d*,*p*)	4.44	1.45	1.21

[a]Scaled by 0.83, which is computed using the ratio of the BSSE-corrected MP2 binding enegy (2.06 kcal/mol) to the CCSD(T) (1.72 kcal/mol) value for the aug-cc-pVDZ basis set.
[b]Not optimized, the geometry is taken from the planar C_6H_6 tilted one-H-atom-down results.

addition of NH_3. We first optimize the structure with C_{3v} symmetry at the MP2/6-31G* level (see Fig. 3). In this structure the C_3 axis of NH_3 is perpendicular to the surface. The N is 3.50 Å above the plane of the carbon atoms. This structure has two imaginary frequencies. Displacing the geometry in the direction of the imaginary modes leads to two minima, which are also shown in Fig. 3; the first has one H atom pointing toward the surface, while the second has two H atoms pointing toward the surface. As is shown in Table I, the one and two-H atoms down conformations are very similar in energy with the one-H down being slightly more stable than the two-H down for the largest basis set.

The tilted structures are more stable than the perpendicular ones, because the bonding is mostly electrostatic in origin. C_6H_6 has a quadrupole moment and NH_3 has both a dipole and quadrupole moment. The dipole-quadrupole interaction favors the NH_3 C_3 axis pointing straight toward the C_6H_6, while the quadrupole-quadrupole interactions favor the NH_3 C_3 axis parallel to the plane of the C_6H_6. The observed tilt is a compromise between these two electrostatic terms.

Previous work[16] reported that NH_3 bonded to the nanotube N end down. It appears that this is also the orientation used in the work of Zhao *et al.*[15], but unfortunately the manuscript is not very clear on this point. Having the N end down is expected to be unfavorable, since both the quadrupole-quadrupole and quadrupole-dipole interactions are repulsive for this orientation. We investigated this orientation for a pyrene ($C_{16}H_{10}$) model of graphite, and while we find a bound system before accounting for BSSE, it is unbound after applying the BSSE correction. If we tilt NH_3 slightly, our final optimized structure is the one with one hydrogen atom down as found for the C_6H_6 model (see Fig. 3). The similar rotation of NH_3 from N down to H down also occurs for the larger $C_{24}H_{12}$ model. Thus we conclude that the configuration with N down is unfavorable, and that the orientations found in the previous calculations have been a result of BSSE. We do not consider this orientation further.

While the bonding is expected to be mostly electrostatic, other factors, such as dispersion, can contribute to the bonding for such weakly bound systems. Since the MP2 approach is known to overestimate the dispersion forces, we perform MP2 and CCSD(T) calculations using the aug-cc-pV double zeta basis set. The MP2/6-31G* one H-down geometry is used in the CCSD(T) calculations. This calibration calculation confirms that the MP2 binding

energy is too large and we use the ratio of the CCSD(T) and MP2 results to scale all of our MP2 results. We optimized the NH_3-C_6H_6 distance using the BSSE corrected aug-cc-pVTZ energies, and we find that the NH_3-C_6H_6 distance increased by less than 0.02 Å and the binding energy is increased by less than 0.01 kcal/mol. Thus, our best estimate for the NH_3 binding to graphite using the C_6H_6 model comes from the scaled aug-cc-pVTZ and is 2.02 kcal/mol.

The next series of calculations also study graphite, but use the larger $C_{24}H_{12}$ model. The geometry is fully optimized starting from NH_3 above the central ring, with the same orientation found for the tilted one H-down NH_3-C_6H_6 system. The final optimized geometry has the C_3 axis of NH_3 perpendicular to the surface. Since $C_{24}H_{12}$ has a larger quadrupole moment than C_6H_6, one might assume that NH_3 would also be tilted. However, the binding energy is larger for $C_{24}H_{12}$ than for C_6H_6 and the N is 0.15 Å closer to the surface; therefore, the NH_3-surface repulsion effects are larger for $C_{24}H_{12}$ than for C_6H_6. $C_{24}H_{12}$ is more polarizable than C_6H_6, which should increase the dipole-induced dipole and the dispersion interactions for $C_{24}H_{12}$ relative to C_6H_6. In addition to these real contributions to the bonding, the BSSE changes with the tilting of NH_3. For a fixed N-surface height, the three H atoms pointing at the surface should have a larger BSSE than the one H atom pointing at the surface. As NH_3 approaches the surface, the BSSE will increase and so should the difference in BSSE between the three H atoms and one H atom pointing toward the surface. Thus, it is possible that as the overall binding increases and NH_3 moves toward the surface, the BSSE can begin to favor the three H atoms down. Since it is possible that the change in the NH_3 orientation was due to BSSE and not due to real changes in the bonding, we performed a single calculation for tilted NH_3 on coronene. In this calculation, the NH_3 geometry and position above the surface were taken from the optimized NH_3-C_6H_6 geometry. The BSSE corrected binding energy of this tilted NH_3-$C_{24}H_{12}$ geometry (1.51 kcal/mol) is larger than the BSSE corrected binding energy (1.26 kcal/mol) of the three-H-atom-down orientation (i.e., the MP2 optimization geometry). The same effect is observed for the larger 6-31G(2*d*,*p*) basis set. This supports our suggestion that the system is probably really tilted, but the energy difference between the one-H-atom down and three-H-atoms down is small.

The largest basis set that we have used for $C_{24}H_{12}$ [6-31G(2*d*,*p*)] yields an NH_3 scaled binding energy of 1.88 kcal/mol for the tilted geometry. The same basis set for C_6H_6 yields 1.13 kcal/mol. Thus, expanding the model of graphite increases the binding energy by 0.75 kcal/mol. Adding this correction onto our best value of 2.02 kcal/mol for C_6H_6 yields our best estimate of 2.77 kcal/mol for the NH_3 binding energy to $C_{24}H_{12}$. As discussed previously[29], the quadrupole moment per carbon atom of C_6H_6 and $C_{24}H_{12}$ is about twice that of graphite, thus the electrostatic contributions to both of our graphite models are expected to be too large. Using the subcomponent dipole and quadrupole moments leads to electrostatic contributions to the binding for NH_3 to C_6H_6 and $C_{24}H_{12}$ of 0.33 and 1.08 kcal/mol, respectively. If we reduce these electrostatic contributions to the bonding by a factor of 2 to account for the models' overestimation of the graphite quadrupole moment, we obtain 1.86 and 2.23 kcal/mol for the C_6H_6 and $C_{24}H_{12}$ models, respectively.

TABLE II. NH_3 binding energy, in kcal/mol, computed using the B3LYP/6-31G* level of theory. The geometry is taken from the ring calculation and not optimized.

Planar C_6H_6	1.37
Planar $C_{24}H_{12}$	1.25
Curved $C_{24}H_{12}$	1.43
Ring	3.54
Full tube (C_{150}) model	0.51

It is well known[30–33] that it is very difficult to compute accurate binding energies for weakly bound molecules. The binding energy without a BSSE correction tends to be larger than the true value, and the value after the BSSE correction tends to be smaller. As the basis set is improved, the BSSE decreases and BSSE-corrected binding energy increases. For our best basis set used for the C_6H_6 model, the BSSE correction is 0.75 kcal/mol. We therefore expect that improving the basis set will increase our C_6H_6 model binding energy by less than 0.75 kcal/mol. However, our graphite binding energy is computed by combining several values, such as a model size and electrostatic correction. Taking these factors into account, we estimate the NH_3 binding to graphite to be 2.0 ± 2.0 kcal/mol. It is difficult to measure the low coverage NH_3 binding energy for graphite, since the NH_3-NH_3 interaction is similar in magnitude to the NH_3-graphite interaction and our value is reasonably consistent with previous theoretical and experimental values.[34]

We now consider models for a (9,0) tube. The first model consists of a curved coronene molecule to represent the surface of the tube, where the positions of the carbon atoms are taken from an optimized tube with two caps (see Fig. 1), while the C-H bonds are taken as colinear with the C-C bonds in the full tube. The NH_3 geometry and position above the $C_{24}H_{12}$ were fully optimized at the MP2/6-31G* level. Like the planar $C_{24}H_{12}$, the C_3 axis of NH_3 is perpendicular to the surface of the tube. The BSSE-corrected MP2 binding energies are summarized in Table I, and NH_3 binding energy of the curved $C_{24}H_{12}$ is about 0.5 kcal/mol smaller than for the planar case. Thus, it might appear that the binding of NH_3 to a (9,0) SWCNT is less than for graphite. However, bending the $C_{24}H_{12}$ changes its quadrupole moment and creates a dipole moment, which reduces the electrostatic bonding. Since a real nanotube will not have a dipole moment, the computed change in NH_3 binding with bending of the $C_{24}H_{12}$ does not truly reflect the difference between graphite and the (9,0) tube. Therefore, by using this model we can conclude that the binding energy for NH_3 on graphite and a (9,0) tube are similar, but we cannot determine this difference accurately.

The growth in computational expense with model size makes it difficult to study models larger than $C_{24}H_{12}$ at the

MP2 level, therefore, we investigate the dependence of the NH_3 binding energy on tube models using the B3LYP/6-31G* level of theory. Before considering tube models, we first consider the C_6H_6 and $C_{24}H_{12}$ models of graphite; the results are summarized in Table II. The B3LYP/6-31G* optimized structure of NH_3-C_6H_6 is similar to the MP2 structure with one H atom tilted down, but the N is 0.35 Å further away from the surface for the B3LYP level. The B3LYP binding energy, not corrected for BSSE, is somewhat smaller than our best estimate for the NH_3-C_6H_6 binding energy. The optimal B3LYP geometry for NH_3-$C_{24}H_{12}$ has the NH_3 C_3 axis perpendicular to the surface, as found for the MP2 level, but the N-surface distance is 0.2 Å longer for the B3LYP than for the MP2. (Note that, like the MP2, this is true even if one starts from a tilted NH_3 geometry.) The B3LYP NH_3-$C_{24}H_{12}$ binding energy is slightly smaller than for the C_6H_6. The binding energy of NH_3 to the curved $C_{24}H_{12}$ is slightly larger than found for the planar case. While these binding energies are similar to those found at the MP2 level, the exact trends are not matched. These results suggest that B3LYP is qualitatively correct and can give some insight into changes in the model with size.

We next consider $C_{72}H_{18}$, which is a ring of a (9,0) nanotube with the dangling C-C bonds terminated with H atoms (see Fig. 1). This nanotube model does not have an unphysical dipole moment as was found for the curved $C_{24}H_{12}$, but the computed binding energy is found to be more than twice that of the curved $C_{24}H_{12}$ model. This large binding energy arises, because the ring has a very large quadruple moment. That is, while this model does not have a nonphysical dipole moment, it has a nonphysical quadrupole moment.

Finally, we consider the C_{150} full tube. These calculations are very large, having 2271 basis functions, and the optimization is very time consuming even running in parallel. This model has removed the nonphysical dipole moment of the curved $C_{24}H_{12}$ model and the nonphysical quadrupole moment of the $C_{72}H_{18}$ ring. The computed NH_3 binding energy is only 0.51 kcal/mol. We suspect that this is a lower bound, as improving the basis set is expected to increase the binding energy. In addition, the B3LYP approach, like most other DFT functionals, does not describe dispersion forces very well[35–37], and in general, significantly underestimating the effect. Thus, one must add on some correction for the van der Waals bonding that is missing in the DFT treatment. Using the difference between the B3LYP binding energies and our best estimates for the MP2 values for the planar models of graphite suggests that the dispersion contribution to the bonding could increase the B3LYP binding energy; for the C_6H_6 model the increase is 0.65 kcal/mol, while the $C_{24}H_{12}$ model suggests an increase of 1.52 kcal/mol. A correction of this magnitude brings the B3LYP full tube value into reasonable agreement with our best estimate of 2.0 ± 2.0 kcal/mol, based on the MP2 calculations of graphite and the assumption that the (9,0) tube and graphite values are similar. These calculations again demonstrate that weakly bound systems are very difficult to treat, since changes in the model can make small absolute changes in the binding energy, which are a sizable fraction of the total binding energy.

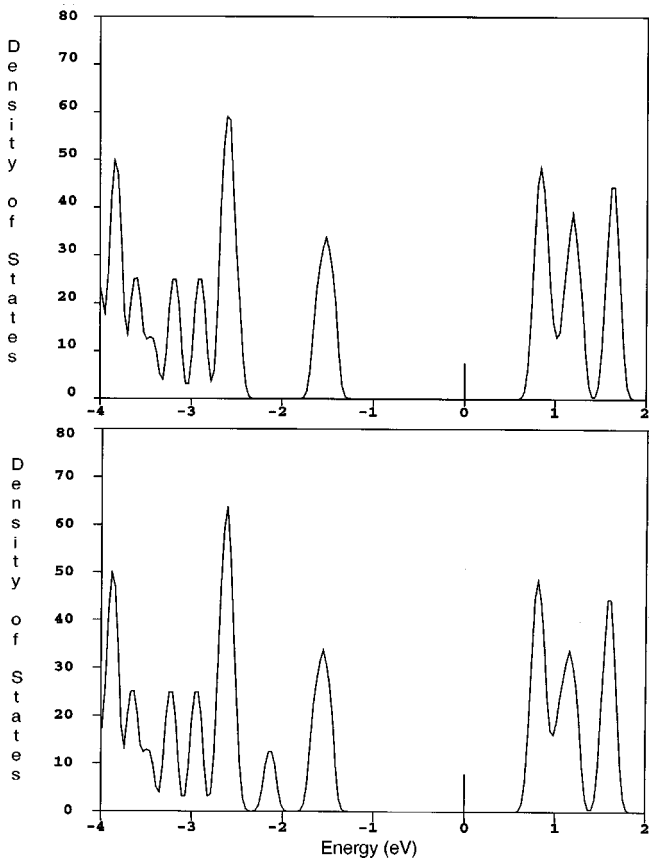

FIG. 4. Electronic density of states computed using four k points and a 0.05-eV Gaussian broadening. The upper plot is for a bare (10,0) tube and the lower plot is for a (10,0) tube interacting with NH_3.

Up to this point we have focused on the orientation and binding energy, however, the experiments actually measure the change in current. One interpretation of the experiments is that there is charge transfer between NH_3 and SWCNT. Our calculations do not support this view; the maximum charge transfer observed in our calculations is 0.008 electrons, which is consistent with the weak bonding. We should note, however, that the NH_3 dipole and quadrupole moment can induce some polarization of the charge on SWCNT. We therefore consider the change in the band structure with the addition of NH_3. (We should note that previous calculations[15,16] considered the band structure, but these are for the wrong orientation of NH_3.) We switch to a (10,0) tube, since this is a semiconductor and one expects a larger change in a semiconductor tube than a conducting tube. In Fig. 4 we present the computed electronic density of states of a bare (10,0) tube and of a (10,0) tube interacting with NH_3. A comparison of the two plots shows that they only differ by a small peak appearing at approximately -2.1 eV, which belongs to an isolated NH_3 molecule. We can conclude that the presence of NH_3 does not modify the density of states of the nanotube and should not lead to a change in the conductivity of the nanotube.

IV. CONCLUSIONS

The calculations show that NH_3 is weakly bound (2 ± 2 kcal) to both graphite and a (9,0) carbon nanotube, with the hydrogen end pointing toward the graphite or carbon nanotube. There is very little charge transfer. Bandstructure calculations show essentially no change in the nanotube band gap when NH_3 is added.

ACKNOWLEDGMENTS

A.R. was supported by Contract No. NAS2-03144 of the University Affiliated Research Center (UARC)/UC Santa Cruz. A.R. would like to acknowledge helpful discussions with Toshishige Yamada.

[1] M. S. Strano, C. B. Huffman, V. C. Moore, M. J. O'Connell, E. H. Haroz, J. Hubbard, M. Miller, K. Rialon, C. Kittrell, S. Ramesh, R. H. Hauge, and R. E. Smalley, J. Phys. Chem. B **107**, 6979 (2003).
[2] A. Goldoni, R. Larciprete, L. Petaccia, and S. Lizzit, J. Am. Chem. Soc. **125**, 11 329 (2003).
[3] A. Ricca and J. A. Drocco, Chem. Phys. Lett. **362**, 217 (2002).
[4] D. C. Sorescu, K. D. Jordan, and Ph. Avouris, J. Phys. Chem. B **105**, 11 227 (2001).
[5] A. Ricca, C. W. Bauschlicher, and A. Maiti, Phys. Rev. B **68**, 035433 (2003).
[6] P. Giannozzi, R. Car, and G. Scoles, J. Chem. Phys. **118**, 1003 (2003).
[7] V. Derycke, R. Martel, J. Appenzeller, and Ph. Avouris, Appl. Phys. Lett. **80**, 2773 (2002).
[8] S. Heinze, J. Tersoff, R. Martel, V. Derycke, J. Appenzeller, and Ph. Avouris, Phys. Rev. Lett. **89**, 106801 (2002).
[9] Ph. Avouris, Acc. Chem. Res. **35**, 1027.(2002)
[10] T. Yamada, Phys. Rev. B **69**, 125408 (2004).
[11] P. G. Collins, K. Bradley, M. Ishigami, and A. Zettl, Science **287**, 1801 (2000).
[12] J. Kong, N. R. Franklin, C. Zhou, M. G. Chapline, S. Peng, K. Cho, and H. Dai, Science **287**, 623 (2000).
[13] K. Bradley, J.-C. P. Gabriel, M. Briman, A. Star, and G. Grüner, Phys. Rev. Lett. **91**, 218301 (2003).
[14] K. Bradley, J.-C. P. Gabriel, A. Star, and G. Grüner, Appl. Phys. Lett. **83**, 3821 (2003).
[15] J. Zhao, A. Buldum, J. Han, and J. P. Lu, Nanotechnology **13**, 195 (2002).
[16] H. Chang, J. D. Lee, S. M. Lee, and Y. H. Lee, Appl. Phys. Lett. **79**, 3863 (2001).
[17] R. J. Bartlett, Annu. Rev. Phys. Chem. **32**, 359 (1981); C. Hampel, K. Peterson, and H.-J. Werner, Chem. Phys. Lett. **190**, 1 (1992).
[18] K. Raghavachari, G. W. Trucks, J. A. Pople, and M. Head-Gordon, Chem. Phys. Lett. **157**, 479 (1989).
[19] P. J. Stephens, F. J. Devlin, C. F. Chabalowski, and M. J. Frisch, J. Phys. Chem. **98**, 11623 (1994).
[20] A. D. Becke, J. Chem. Phys. **98**, 5648 (1993).
[21] M. J. Frisch, J. A. Pople, and J. S. Binkley, J. Chem. Phys. **80**, 3265 (1984) and references therein.
[22] T. H. Dunning, J. Chem. Phys. **90**, 1007 (1989).
[23] R. A. Kendall, T. H. Dunning, and R. J. Harrison, J. Chem. Phys. **96**, 6796 (1992).
[24] GAUSSIAN98, Revision A.11, M. J. Frisch *et al.*, Gaussian, Pittsburgh, PA , 1998.
[25] MOLPRO is a package of *ab initio* programs written by H.-J. Werner and P. J. Knowles, with contributions from J. Almlöf, R. D. Amos, A. Berning, D. L. Cooper, M. J. O. Deegan, A. J. Dobbyn, F. Eckert, S. T. Elbert, C. Hampel, R. Lindh, A. W. Llyod, W. Meyer, A. Nicklass, K. Peterson, R. Pitzer, A. J. Stone, P. R. Taylor, M. E. Mura, P. Pulay, M. Schütz, H. Stoll, and T. Thorseinsson.
[26] Accelrys Inc., CASTEP Users Guide, San Diego, 2001.
[27] V. Milman, B. Winkler, J. A. White, C. J. Pickard, M. C. Payne, E. V. Akhmatskaya, and R. H. Nobes, Int. J. Quantum Chem. **77**, 895 (2000).
[28] J. P. Perdew, K. Burke, and M. Ernzerhof, Phys. Rev. Lett. **77**, 3865 (1996).
[29] M. Cinke, J. Li, C. W. Bauschlicher, A. Ricca, and M. Meyyappan, Chem. Phys. Lett. **376**, 761 (2003).
[30] H. Partridge and C. W. Bauschlicher, Mol. Phys. **96**, 705 (1999).
[31] F.-M. Tao and Y.-K. Pan, J. Chem. Phys. **97**, 4989 (1992).
[32] W. Klopper and J. Noga, J. Chem. Phys. **103**, 6127 (1995).
[33] D. E. Woon, J. Chem. Phys. **100**, 2838 (1994).
[34] P. Rowntree, G. Scoles, and J. Xu, J. Chem. Phys. **92**, 3853 (1990).
[35] S. Tsuzuki and H. P. Lüthi, J. Chem. Phys. **114**, 3949 (2001).
[36] X. Wu, M. C. Vargas, S. Nayak, V. Lotrich, and G. Scoles, J. Chem. Phys. **115**, 8748 (2001).
[37] U. Zimmerli, M. Parrinello, and P. Koumoutsakos, J. Chem. Phys. **120**, 2693 (2004).